Environ Res Tec, Vol. 8, Issue. 1, pp. 65–72, March 2025

Environmental Research and Technology
https://dergipark.org.tr/tr/pub/ert
DOI: https://10.35208/ert.1477303

Environmental Research & Technology

Research Article

Removal of sodium isopropyl xanthate by capacitive deionization process

Yasemin ÖZTÜRK*

Department of Mining Engineering, Hacettepe University, Ankara, Türkiye

ARTICLE INFO

Article history
Received: 02 May 2024
Revised: 27 July 2024
Accepted: 29 July 2024

Key words:
Capacitive deionization (CDI); Electrochemical advanced oxidation processes (EAOPs); Flotation; Residual xanthate; Water treatment

ABSTRACT

This study investigated the removal of sodium isopropyl xanthate (SIPX) by capacitive deionization using an ion exchange resin/PVDF electrode. The electrode was prepared by coating a layer of ion exchange resin (Amberlite FPA54) and polyvinylidene fluoride (PVDF) on the carbon electrode. Batch experiments demonstrated that 96% of SIPX was removed through electrosorption and electrochemical advanced oxidation processes at 1 V. Carbon disulfide (CS_2) was generated as a by-product of the xanthate oxidation. Adsorption/desorption cycle tests revealed that the ion exchange resin/PVDF electrode has high adsorption capacity, and the maximum adsorption could not be achieved within 60 min of adsorption times. The total xanthate removed in the final adsorption stage of eight cycles was 323 mg/m^2, corresponding to 34.1% of xanthate from a 20 mg/L xanthate solution that flowed 0.4 mL per min at 1 V for 60 min of adsorption. At the end of the 30 min. desorption, 32.1% of the adsorbed xanthate was released back into the solution and oxidized to CS_2, which was adsorbed by the electrodes in the following adsorption stage. The percentage of the concentrate flow at the end of the desorption stage was 33%. The findings of the study suggest that CDI is a promising tool for the mining industry. However, further research is needed to evaluate its efficiency for specific mining applications.

Cite this article as: Öztürk Y. Removal of sodium isopropyl xanthate by capacitive deionization process. Environ Res Tec 2025;8(1)65–72.

INTRODUCTION

Mineral processing operations consume significant amounts of water. Mining represents a small fraction of total water use worldwide but has a major effect on the quantity and quality of water resources at mine sites [1]. Environmental concerns have led to the need to reuse water to conserve freshwater resources [2].

Froth flotation is the most water intensive process in mining operations due to the significant water usage involved. However, among the other mineral processing methods it is the most affected by water quality [3]. Water reuse in flotation results in the accumulation of dissolved compounds that change the chemistry of the system and often have a detrimental effect on recovery and grade [4].

Xanthates are common collectors used in the flotation of sulphide minerals. They are not stable. Upon oxidation and hydrolysis, they form species such as perxanthate, monothiocarbonate, and dixanthogen, which affect the action of the collector [5]. In addition, the remaining xanthate and its degradation compounds in the process water can reduce the selectivity among minerals [4]. Although many flotation plants reuse tailings water at high levels, some discharge may occur. Without proper treatment, releases to the environment can result in contamination of water resources at the mine site. This study offers a novel and effective method for the removal of xanthate, aiming to reduce environmental impacts and conserve water resources.

In the last decade, xanthate removal via chemical oxidation using ozone [6], hydrogen peroxide, Fenton, and solar pho-

***Corresponding author.**
*E-mail address: yozdil@hacettepe.edu.tr

tofenton processes [7], biodegradation [8], and adsorption by bentonite [9], montmorillonites [10], and activated carbon [11] have been extensively studied. The drawbacks of conventional methods, such as high reagent consumption, slow removal rate, and by-product formation, have led to the investigation of treatment methods that reduce xanthate to small molecules such as CO_2, H_2O, and SO_4^{2-}. For this purpose, the electrochemical advanced oxidation process, which utilizes very powerful oxidizing hydroxyl radicals (·OH), was employed to eliminate xanthate from flotation water. During the process, 95% of the xanthate was removed by producing carbon disulfide as an oxidation product, which was removed by the electrodes to some extent [12].

Electrosorption, also known as capacitive deionization (CDI), is a two-stage desalination process; the first stage is an ion electrosorption process that immobilizes ions on pairs of carbon electrodes to purify water. The second stage is the regeneration of the electrodes through the release of the adsorbed ions [13]. CDI has recently become an energy-efficient and cost-effective water treatment method as it requires lower operational voltages than other technologies such as reverse osmosis (RO), electrodialysis (ED), and distillation. Besides, unlike membrane-based methods such as RO and nanofiltration, CDI does not require the use of high-pressure pumps or membranes [14]. The energy demand of the CDI process is approximately 0.1–1.5 kWh/m^3, depending on the influent concentration and the effluent requirements. On the other hand, the typical energy requirement for RO treatment of feed water with a salinity of less than 5 g/L is about 0.8–2.5 kWh/m^3. Other emerging technologies, such as membrane CDI (MCDI) and flow-electrode CDI (FCDI), can further improve the energy efficiency of treatment compared to CDI [15].

Activated carbon (AC) is a viable electrode material due to its characteristic properties such as high pore volume, pore size, and pore connectivity, in addition to electronic conductivity and electrochemical stability. However, it has several limitations impeding its desalination capacity [16]. Various studies in the literature have shown that combining AC with other materials improves its desalination performance. For instance, adding ion exchange resin to the electrode improved performance by 35% due to increased hydrophilicity [17]. The anion exchange resin/QPVA coated carbon electrode removed sulfate selectively [18]. The AC electrode loaded with titanium dioxide improved the desalination performance by 62.7% [19]. Reduced graphene oxide and activated carbon composite (GAC) is a promising material with higher electrosorption capacity mainly based on the advantages of graphene acting as a bridge to form a conductive network, that prevents the aggregation of AC [20].

This study investigated the removal of SIPX by capacitive deionization. An electrochemical cell was fabricated using a carbon electrode coated with an ion exchange resin/PVDF layer as the anode and a cation exchange membrane attached to the carbon electrode as the cathode. The fabrication and characterization of the resin/PVDF electrode are presented here. The process efficiency was evaluated by batch and continuous flow experiments.

Table 1. Characteristics of the ion exchange resin*

	Amberlite FPA54
Copolymer	Crosslinked phenol-formaldehyde polycondensate
Matrix	Highly porous
Functional group	Tertiary amine
Physical form	Gray, opaque, granules
Ionic form as shipped	Free base
Total exchane capacity	≥1.8 Eq/L
Water retention capacity	60–65%
Particle size	470–740 µm

*Manufacturer supplied.

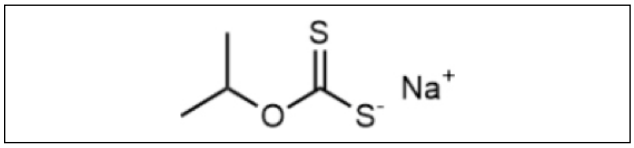

Figure 1. Structural formula of sodium isopropyl xanthate (SIPX).

MATERIALS AND METHODS

Powdered activated carbon (PAC; CEP-21K, PCT Co., surface area of 2040 m^2/g) was used to fabricate electrodes. A cation exchange membrane with an exchange capacity of 2.0 mol/kg was received from Shanghai Shanghua, LLC. A weak base anion exchange resin (Amberlite FPA-54) was purchased from DOW. Characteristics of the ion exchange resin are given in Table 1. Polyvinylidene fluoride (PVDF, molecular weight: 534,000 g/mol) and N, N-Dimethylformamide (DMF, ≥99.8%) were obtained from Sigma Aldrich. Sodium isopropyl xanthate (SIPX) was provided by a commercial supplier. The structural formula of SIPX is presented in Figure 1.

Preparation and Characterization of Electrodes

The carbon electrodes consisted of 90% PAC and 10% PVDF binder, based on the total electrode mass. The preparation of the electrodes consisted of three main steps: preparing the slurry, casting, and drying. To prepare the slurry, PVDF was dissolved in DMF (4%) by mixing for 1 hour. After complete dissolution, PAC was added to be 90% of the total mass. The resulting mixture (30% solids) was stirred overnight for homogenization. The carbon slurry was then cast onto the graphite sheet with a thickness of 300 µm using a flow coater (Newport, USA). The electrodes were dried at room temperature after deposition.

Ion exchange resin, AMBERLITE FPA54 was used to fabricate anode by casting a layer of PVDF and grounded resin on the carbon electrode surface. To prepare the slurry AMBERLITE FPA54 resin was grinded by mortar grinder (Retsch RM200, Retsch Gmbh, Germany). The ion exchange resin powder was mixed with 10% PVDF at a 1:1

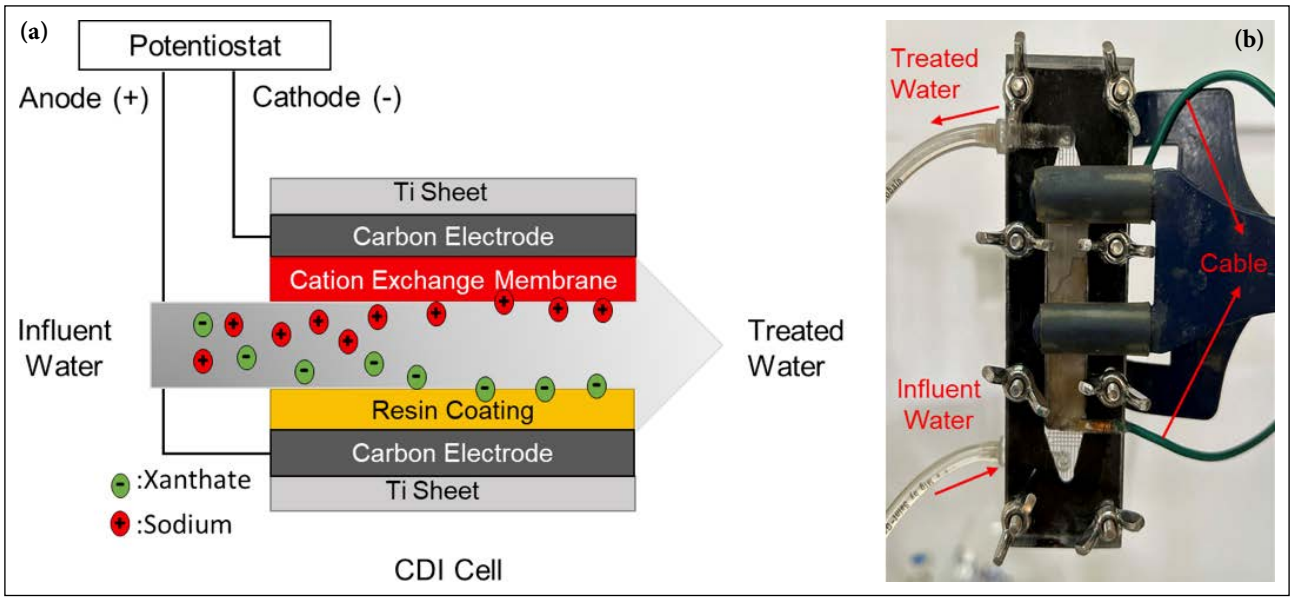

Figure 2. Schematic diagram of bench-scale desalination test setup [13] **(a)** and photograph of the CDI cell **(b)**.

resin to PVDF ratio. Ion exchange resin/PVDF slurry was deposited on the carbon electrode with a thickness of 30 µm and dried at room temperature.

The size of ground resin was measured by dynamic light scattering using a Zetasizer (Brookhaven, OMNI, USA). The surface and cross-sectional morphologies of the ion exchange resin/PVDF electrode were characterized by scanning electron microscopy (TESCAN, GAIA3, Triglav, Brno, Czech Republic).

Desalination Experiments

A schematic representation of the bench-scale capacitive deionization test setup is given in Figure 2. The feed solution was pumped with a peristaltic pump (Cole Parmer, Masterflex, LS Easy Load 7518–00, USA) through a flow by type capacitive deionization cell. A potential was applied by using a potentiostat (Gamry PCI-4750, Warminster, PA, USA) during the process. pH of the effluent solution was measured. The CDI cell consisted of two electrodes, an ion exchange resin/PVDF coated carbon electrode as the anode, and a cation exchange membrane placed on top of the carbon electrode as the cathode. The size of the electrode was 10X50 mm. The electrodes were separated from each other by a non-conductive nylon separator. In all experiments, the flow rate of the solution was 0.4 mL per minute.

Batch electrosorption tests were conducted to observe the xanthate removal efficiency by capacitive deionization. 20 ml SIPX solution at various concentrations; 10 mg/L, 50 mg/L, and 100 mg/L was cycled through the CDI test setup for 24 hours at 1 V. The final concentration of the solution was measured by UV-Vis spectrophotometer (Multispect 1501, Shimadzu, Kyoto, Japan) to determine the concentration of residual SIPX.

Continuous flow tests were performed for adsorption/desorption periods of 60 minutes and 30 minutes, respectively. The influent concentration of SIPX solution was 20 mg/L. The operating voltage was set to 1 V for adsorption and -10 V for desorption. A multi-step potential method was used to maintain a constant voltage during operation by potentiostat. Effluent samples were collected continuously at 10 min. intervals for adsorption and 3 min. intervals for desorption for the determination of SIPX by UV-Vis spectrophotometer. Four adsorption and desorption cycles were conducted before sampling, and then data collection began for four cycles after ensuring the system had reached a dynamic steady state.

Process efficiency was determined by the amount of total salt removed (SR, mg/m^2 (eq1)) and salt removal efficiency % (SRE %, (eq2)) during the adsorption stage.

$$SR = \frac{Q\int_0^t (C_i - C_f)dt}{A_e} \quad (1)$$

$$SRE[\%] = \frac{\int (C_i - C_f)d_t}{C_i t} x100\% \quad (2)$$

Q: flow rate (L/s); Ci: initial concentration (mg/L); Cf: final concentration (mg/L); t: time (s); Ae: effective frontal area of the anode (m^2).

Cost Analysis

The energy consumption for the adsorption and desorption steps was approximately determined using eq3 [21].

$$Energy\ Demand\ for\ Ads.and\ Des.= \left(\frac{kWh}{m^3}\right) = \left(a\frac{I_{ads.}V_{ads.}}{Q}\right) + \left(b\frac{I_{des.}V_{des.}}{Q}\right) \quad (3)$$

Iads: average current for adsorption (A); Vads: average voltage for adsorption (V); Ides: average current for desorption (A); Vdes: average voltage for desorption (V); Q: flow rate (m^3/h); a: water recovery rate; b: concentrate flow rate.

The unit price of electricity ($0.08/kWh in US Dollars) provided by the Turkish Electricity Distribution Corporation was used to convert energy consumption into cost [22].

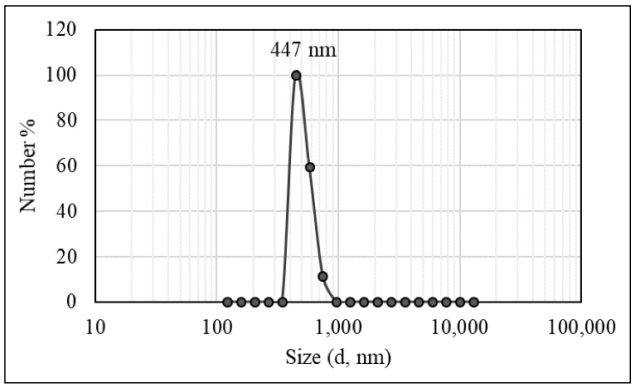

Figure 3. Size distribution of resin powder after grinding.

RESULTS AND DISCUSSION

Characteristics of the Resin/PVDF Electrode

Figure 3 illustrates the size distribution of the resin powder after grinding, with an average particle diameter of 447 nm. The SEM images of the resin/PVDF electrode surface and cross-section given in Figure 4 demonstrated a uniform distribution of resin nanoparticles. They showed that the thickness of the carbon layer was approximately 195 µm. Resin/PVDF coating resulted in a dense surface with a thickness of ~38 µm. The size of the resin particles varied between 0.2 µm and 0.6 µm (Fig. 4).

Desalination Experiments

20 ml of SIPX solution with three different concentrations of 10 mg/L, 50 mg/L, and 100 mg/L was recycled through the CDI cell at a flow rate of 0.4 mL/min and 1 V for 24 hours. The UV spectra of the effluent solutions are presented in Figure 5. Absorptions at 226 nm and 301 nm corresponded to residual xanthate in the effluent. The concentrations of SIPX in the effluent were 0.94 mg/L, 2.59 mg/L, and 4.46 mg/L for the 10 mg/L, 50 mg/L, and 100 mg/L influent solutions, respectively.

In acidic media, water discharges on the electrode, leading to the production of hydroxyl radicals (·OH) on the electrode surface (eq4). These radicals facilitate the electrochemical oxidation of organic compounds. The electrochemical oxidation of an organic compound by ·OH then occurs on the anode surface (eq 5) [23].

$$M+H_2O \rightarrow M(\cdot OH)+H^+ +e^- \quad (4)$$

$$M(\cdot OH)+R \rightarrow M+OxidationProducts+H^+ +e^- \quad (5)$$

M: the electrode, R: the organic compound.

A peak was detected at 206 nm in the UV spectra of 50 mg/L and 100 mg/L SIPX solutions (Fig. 5). It indicated the formation of carbon disulfide (CS_2) [24] by electrochemical oxidation of the -CSS- group of the xanthate by hydroxyl radicals during the process [6]. The CS_2 peak was not detected in the UV spectrum at an influent xanthate concentration of 10 mg/L due to the absorption of the released CS_2 by the electrode. As the initial xanthate concentration increased to 50 mg/L and 100 mg/L, the amount of carbon disulfide in the effluent increased since the resin/PVDF electrode reached its maximum absorption capacity.

Total xanthate removal was 3800 mg xanthate per m^2 of electrode in 20 mL of 100 mg/L SIPX solution. For solutions containing 10 mg/L, 50 mg/L, and 100 mg/L SIPX, 91%, 95%, and 96% of the xanthate was removed, respectively.

Adsorption/desorption cycle tests were performed with 60 min. adsorption and 30 min. desorption phases for eight cycles to investigate the removal efficiency of xanthate from

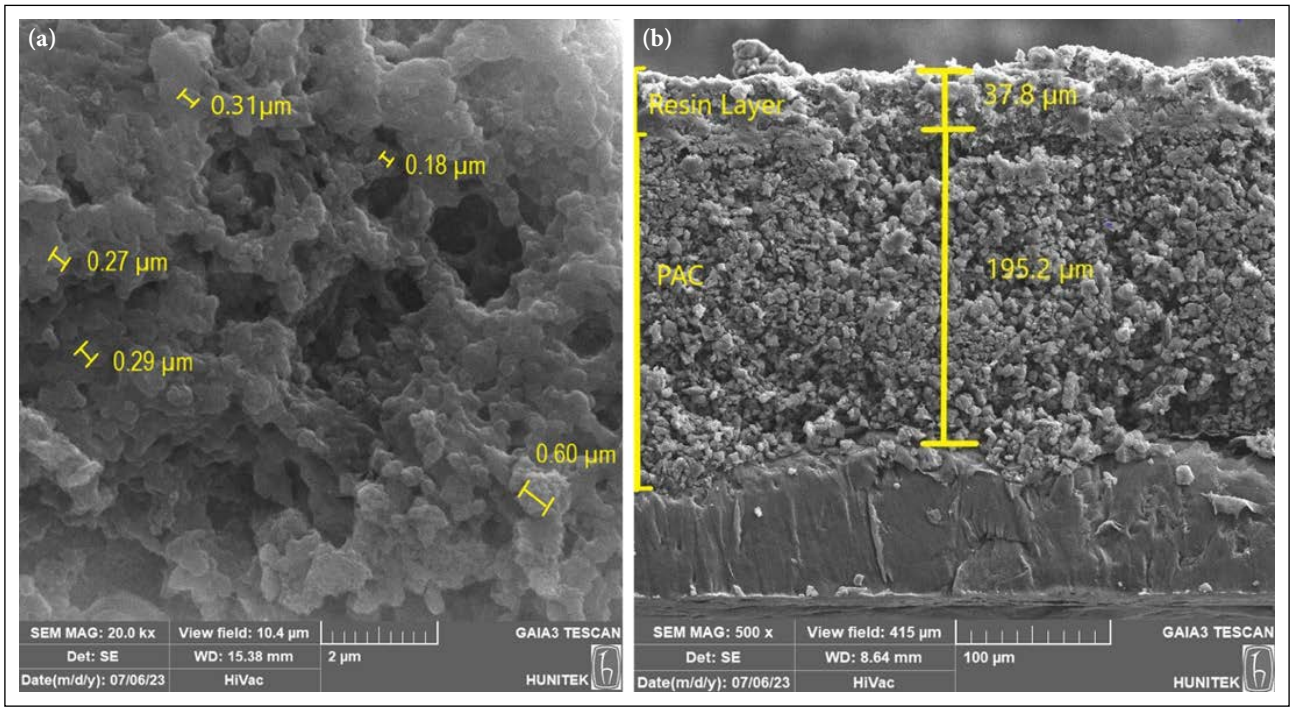

Figure 4. SEM images of surface **(a)** and cross-section **(b)** of resin/PVDF electrode.

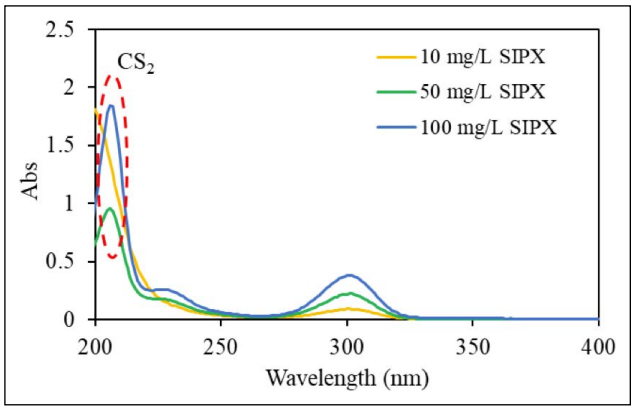

Figure 5. UV spectra for 20 mL SIPX solutions with the initial concentrations of 10 mg/L, 50 mg/L and 100 mg/L after batch electrosorption for 24 h at 1V.

the initial concentration of 20 mg/L SIPX solution. The applied voltage was set to 1 V for adsorption and -10 V for desorption stages. The xanthate solution was continuously passed through the system at a flow rate of 0.4 mL/min.

The UV spectra of the final adsorption/desorption cycle are illustrated in Figure 6. According to the results presented in Figure 6a, the xanthate peak at 301 nm decreased with time, indicating that SIPX was removed during the 60 min. adsorption step. The concentration of SIPX reduced from 20 mg/L to 12.5 mg/L at the end of the adsorption stage. An absorption peak at 206 nm was detected in the effluent sample collected during the first 10 min. of the adsorption stage (A-10 min.), which could be attributed to the formation of CS_2 during the desorption step in the previous cycle [12].

In the desorption stage, the compounds adsorbed by the electrodes were released back into the solution. It was clearly shown that the amount of xanthate and carbon disulfide increased during 30 min. of the desorption stage resulting in the regeneration of the electrode surface (Fig. 6b).

Changes in SIPX concentration during 60 min. adsorption and 30 min. desorption times for the last four adsorption/desorption cycles were given in Figure 7. Based on the results, it can be concluded that the resin/PVDF electrode had a high adsorption capacity and did not reach its maximum adsorption during 60 min. of adsorption step. Some of the xanthate adsorbed on the electrode surface during the adsorption stage was desorbed in the 30 min. desorption stage, but complete desorption could not be achieved.

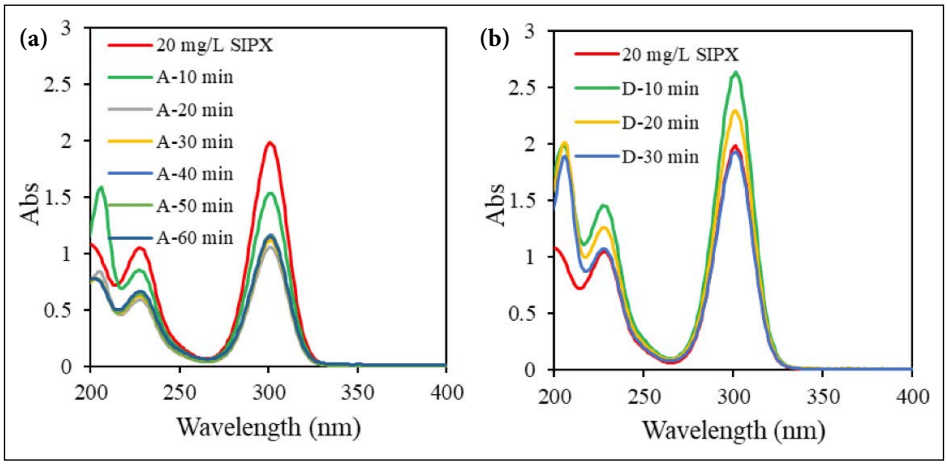

Figure 6. UV-spectra of the final adsorption/desorption cycle for the initial concentrations of 20 mg/L SIPX; a) 60 min. of adsorption times at 1 V and b) 30 min. of desorption times at -10 V

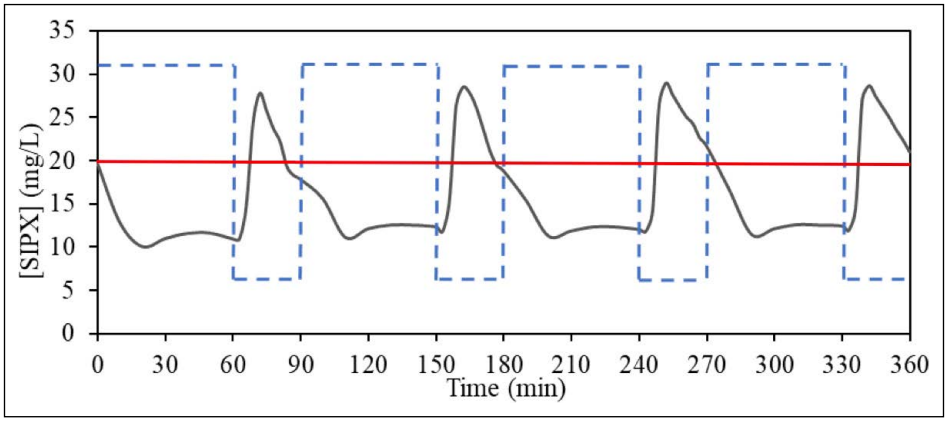

Figure 7. Changes in SIPX concentration during 60 min. adsorption and 30 min. desorption times for the last four adsorption/desorption cycles at an influent concentration of 20 mg/L.

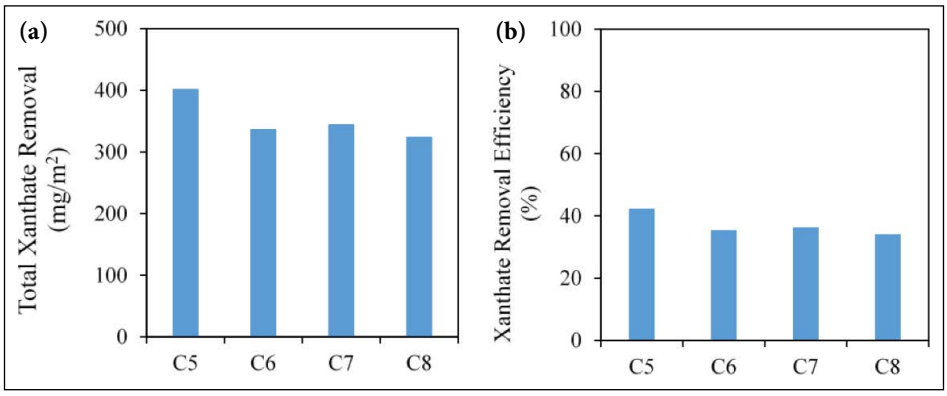

Figure 8. Desalination performance of the electrode; **(a)** total xanthate removal and **(b)** xanthate removal efficiency during 60 min. adsorption times for the last four adsorption cycles at an influent concentration of 20 mg/L SIPX.

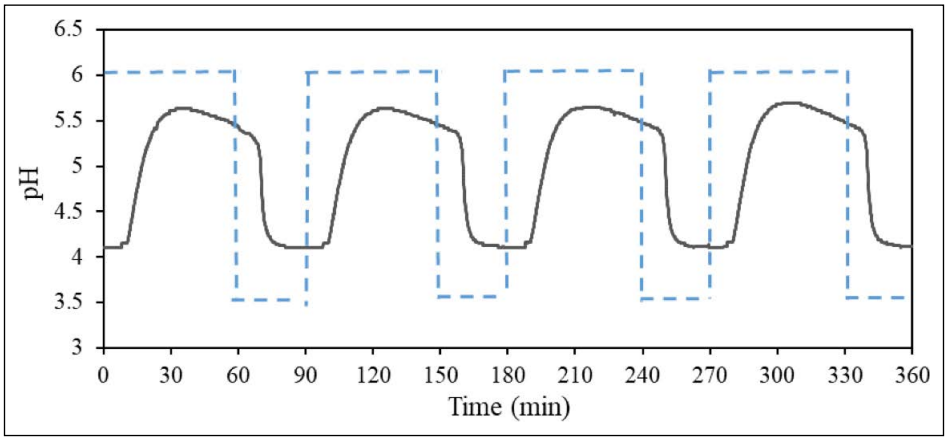

Figure 9. Changes in pH during 60 min. adsorption and 30 min. desorption times for the last four adsorption/desorption cycles at an influent concentration of 20 mg/L SIPX.

The desalination performance of the resin/PVDF coated electrode was assessed by the amount of total xanthate removal and xanthate removal efficiency % during the adsorption stage. Figure 8 illustrates the desalination performance of the electrode during the process. According to the results presented in Figure 8a, in the fifth adsorption cycle, 401 mg/m^2 of xanthate was removed, while in the last cycle, it decreased to 323 mg/m^2, corresponding to 42% to 34.1% of xanthate removal (Fig. 8b). The water recovery for the final adsorption stage was 67%. At the end of the 30 minutes of desorption in the last cycle, 103.9 mg/m^2 of the xanthate was recovered, corresponding to 32.1% xanthate recovery. The percentage of concentrate flow at the end of the final desorption stage was 33%.

Changes in pH during adsorption/desorption cycles were monitored online during the treatment and the results were presented in Figure 9. The pH of the initial solution was measured as 5.39. During the desorption stage, the pH decreased to 4.11, which was attributed to the production of hydroxyl radicals, resulting in the electrochemical oxidation of xanthate to CS_2 [25].

Cost Analysis

In this study, cost analysis was conducted by considering the energy consumption during both the adsorption and desorption stages. The average applied voltage and current were utilized to calculate the energy requirements for the process. During the adsorption phase, a voltage of 1.0 V and a current of 0.23 mA were observed. In the desorption phase, a voltage of -10 V and a current of 1.07 mA were measured.

The cost analysis indicated that the energy demand for the treatment was 0.154 kWh/m^3, corresponding to a cost of 0.013 \$/m^3. This demonstrates that capacitive deionization, known for its cost-effectiveness and low energy consumption in the range of 0.1 to 1.5 kWh/m^3 [15], is highly effective in removing xanthate.

CONCLUSION

The results obtained from this study are summarized below:

- Batch experiments showed that 96% of xanthate corresponded to the 3800 mg xanthate per m^2 of the electrode, which was removed from 20 mL of 100 mg/L xanthate solution that flowed 0.4 mL per minute at 1 V for 24 h via electrosorption and electrochemical advanced oxidation processes.
- Carbon disulfide (CS_2) was generated as a by-product of xanthate oxidation and was adsorbed to some extent by the electrode.

- Both batch and cycle tests demonstrated that the ion exchange resin/PVDF electrode possesses a high adsorption capacity. However, maximum adsorption was not reached within 60 minutes.
- The amount of xanthate removed over the last four adsorption cycles decreased from 401 mg/m^2 to 323 mg/m^2, which corresponds to 42% to 34.1% of xanthate removal.
- At the end of the desorption stage, 32.1% of the adsorbed xanthate was released back into the solution and oxidized to CS_2.
- The pH of the initial solution decreased due to the production of ·OH during the desorption stage.
- The impact of operating parameters such as adsorption/desorption cycle times, applied voltage, and flow rate on desalination performance should be further investigated to improve the process.
- CDI is promising for long-term desalination, but the electrodes may degrade over time. Therefore, the long-term performance of the resin/PVDF electrode should be monitored to determine the overall performance of the process.
- The study highlights CDI's potential for long-term desalination in the mining industry but also notes that the electrodes may degrade over time. Future research should focus on optimizing operating parameters such as adsorption/desorption cycle times, applied voltage, and flow rate to enhance process efficiency. Additionally, the long-term performance and stability of the resin/PVDF electrodes should be monitored to assess their overall efficacy in practical applications.

ACKNOWLEDGEMENTS

The author would like to thank Dr. Evren Çubukçu and Boğaç Kılıçarslan for SEM imaging (Hacettepe University Advanced Technologies Research and Application Center, HUNITEK, Ankara, Türkiye).

DATA AVAILABILITY STATEMENT

The author confirm that the data that supports the findings of this study are available within the article. Raw data that support the finding of this study are available from the corresponding author, upon reasonable request.

CONFLICT OF INTEREST

The author declared no potential conflicts of interest with respect to the research, authorship, and/or publication of this article.

USE OF AI FOR WRITING ASSISTANCE

Not declared.

ETHICS

There are no ethical issues with the publication of this manuscript.

REFERENCES

[1] S. Meißner, "The impact of metal mining on global water stress and regional carrying capacities-a gis-based water impact assessment," Resources, Vol. 10, Article 120, 2021. [CrossRef]

[2] K. A. Slatter, N. D. Plint, M. Cole, V. Dilsook, D. De Vaux, N. Palm, and B. Oostendorp, "Water management in Anglo Platinum process operations: effects of water quality on process operations," in: Proceedings of the International Mine Water Conference. Pretoria, South Africa; 46-55, 2009.

[3] K. Witecki, I. Polowczyk, P. B. Kowalczuk, "Chemistry of wastewater circuits in mineral processing industry-A review," Journal of Water Process Engineering, Vol. 45, Article 102509, 2022. [CrossRef]

[4] S. R. Rao, and J. A. Finch, "A review of water re-use in flotation," Minerals Engineering, Vol. 2, pp. 65-85, 1989. [CrossRef]

[5] M. A. Elizondo-Álvarez, A. Uribe-Salas, and S. Bello-Teodoro, "Chemical stability of xanthates, dithiophosphinates and hydroxamic acids in aqueous solutions and their environmental implications," Ecotoxicology and Environmental Safety, Vol. 207, Article 111509, 2021. [CrossRef]

[6] R. Liu, W. Sun, K. Ouyang, L. Zhang, and Y. Hu Y. "Decomposition of sodium butyl xanthate (SBX) in aqueous solution by means of OCF: Ozonator combined with flotator," Minerals Engineering, Vol. 70, pp. 222-227, 2015. [CrossRef]

[7] B. García-Leiva, L. A. C. Teixeira, and M. L. Torem, "Degradation of xanthate in waters by hydrogen peroxide, fenton and simulated solar photo-fenton processes," Journal of Materials Research and Technology, Vol. 8(6), pp. 5698-5706, 2019. [CrossRef]

[8] S. Chen, W. Gong, G. Mei, Q. Zhou, C. Bai, and N. Xu, "Primary biodegradation of sulfide mineral flotation collectors," Minerals Engineering, Vol. 24, pp. 953-955, 2011. [CrossRef]

[9] R. Rezaei, M. Massinaei, and A. Z. Moghaddam, "Removal of the residual xanthate from flotation plant tailings using modified bentonite," Minerals Engineering, Vol. 119, pp. 1-10, 2018. [CrossRef]

[10] Q. Huang, X. Li, S. Rena, and W. Luo, "Removal of ethyl, isobutyl, and isoamyl xanthates using cationic gemini surfactant modified montmorillonites," Colloids and Surfaces A: Physicochemical and Engineering Aspects, Vol. 580, Article 123723, 2019. [CrossRef]

[11] Y. Ozturk, O. Bicak, and Z. Ekmekci, "Effects of residual xanthate on flotation efficiency of a cu-zn sulfide ore," Minerals, Vol. 12, Article 279, 2022. [CrossRef]

[12] Y. Ozturk, "Electrochemical advanced oxidation for removal of xanthate from flotation process water," Minerals Engineering, Vol. 202, Article 108308, 2023. [CrossRef]

[13] S. Porada, R. Zhao, A. Van der Wal, V. Presser, and P. M. Biesheuvel, "Review on the science and technology of water desalination by capacitive deionization," Progress in Materials Science, Vol. 58, pp. 1388-1442, 2013. [CrossRef]

[14] Y. Oren, "Capacitive deionization (CDI) for desalination and water treatment - past, present and future (a review)," Desalination, Vol. 228, pp. 10-29, 2008. [CrossRef]

[15] S. Y. Pan, A. Z. Haddad, A. Kumar, and S. W. Wang, "Brackish water desalination using reverse osmosis and capacitive deionization at the water energy nexus," Water Research, Vol. 183, Article 116064, 2020. [CrossRef]

[16] M. Tauk, G. Folaranmi, M. Cretin, M. Bechelany, P. Sistat, C. Zhang, and F. Zaviska, "Recent advances in capacitive deionization: A comprehensive review on electrode materials.," Journal of Environmental Chemical Engineering, Vol. 11(6), Article 111368, 2023. [CrossRef]

[17] J. B. Lee, K. K. Parka, S. W. Yoona, P. Y. Parka, K. Parka, and C. W. Lee, "Desalination performance of a carbon-based composite electrode, Desalination, Vol. 237, pp. 155-161, 2019. [CrossRef]

[18] K. Zuo, J. Kim, A. Jain, T. Wang, R. Verduzco, M. Long, and Q. Li, "Novel composite electrodes for selective removal of sulfate by the capacitive deionization process," Environmental Science and Technology, Vol. 52, pp. 9486-9494, 2018. [CrossRef]

[19] L. M. Chang, X. Y. Duan, and W. Liu, "Preparation and electrosorption desalination performance of activated carbon electrode with titania," Desalination, Vol. 270, pp. 285-290, 2011. [CrossRef]

[20] H. Li, L. Pan, C. Nie, Y. Liu, and Z. Sun, "Reduced graphene oxide and activated carbon composites for capacitive deionization," Journal of Material Chemistry, Vol. 22, Article 15556, 2012. [CrossRef]

[21] H. İ. Uzun, and E. Debik, "Economic evaluation of fluoride removal by membrane capacitive deionization," Environmental Research and Technology, Vol. 4(4), 352-357, 2021. [CrossRef]

[22] EPİAŞ Şeffaflık Platformu, https://seffaflik.epias.com.tr/electricity/electricity-markets/day-ahead-market-dam/market-clearing-price-mcp Accessed on Jul 26, 2024

[23] J. Xie, C. Zhang, and T. D. Waite, "Hydroxyl radicals in anodic oxidation systems: generation, identification and quantification," Water Research, Vol. 217, Article 118425, 2022. [CrossRef]

[24] Z. Sun, and W. Forsling, "The degradation kinetics of ethyl-xanthate as a function of pH in aqueous solution," Minerals Engineering, Vol. 10(4), pp. 389-400, 1997. [CrossRef]

[25] B. K. Körbahti, and M. C. Erdem, "Ph change in electrochemical oxidation of imidacloprid pesticide using boron-doped diamond electrodes," Turkish Journal of Engineering, Vol. 1(1), pp. 32-36, 2017. [CrossRef]